Proceedings of the 10th World Congress on Electrical Engineering and Computer Systems and Sciences (EECSS'24)
Barcelona, Spain – August 19 - 21, 2024
Paper No. ICBES 148
DOI: 10.11159/icbes24.148

Spectral EEG Microstates for Detection of Mental Disorders

Vladimir da Rocha Cordeiro Junior[1], Patrick Marques Ciarelli[1]
[1]Universidade Federal do Espírito Santo/Department of Electrical Engineering
Vitória, Brazil
vladimir.cordeiro@edu.ufes.br; patrick.ciarelli@ufes.br

Abstract **-** The present work proposes a novel approach for automatic detection of patients with mental disorder using EEG microstates based on the fundamentals of spectral clustering. This approach involves microstates yielded from Laplacian matrices and its feature extraction, like coverage, individual frequency, duration and shifting frequency, followed by machine learning classification. Using the EEG signals of the TUH Abnormal corpus, which has data from mental disorder patients and healthy subjects, we achieved results that have demonstrated the potential of the technique to efficiently encompass the information present in the EEG and reduce its dimensionality , turning it simpler for straightforward classification. The experiments have presented the minimum mean error of 12.50%, yet many possibilities for new approaches over the processed data with this technique.

Keywords**:** EEG, Microstates, Spectral Clustering, Pairwise, Classification

1. Introduction

Early and objective diagnosis for mental disorders may significantly reduce the impairment to the social aspect and health of the affected subjects, however, the diagnosis is traditionally based on observations and complaints reported by patients or informants, interpreted by specialist [1]. Therefore, the search for neurophysiological biomarkers has gained attention in the last four decades [2][3] and several research have demonstrated promising broads in mental disorders identification using Machine Learning (ML) and Deep Learning (DL) models, leading to prominent biomarkers [1][4][5]. The Electroencephalogram (EEG) signal is one of the most important sources of brain dynamical behavior, due to its high time resolution, low cost, and non-invasive nature [1][6], it has aroused interest as a neurophysiological biomarker.

Brain electric fields captured over the scalp using EEG devices can be used to produce potential topographic maps, whose shifting configurations reveal dynamic patterns associated with the cognitive process, as explored in [2][7]. Later, this way of analyzing EEG signal was related to several cognitive disorders and neurological diseases, such as Attention Deficit Hyperactivity Disorder (ADHD) [4], Multiple Sclerosis [8], and Major Depressive Disorder (MDD) [9]. These topographic electric potential are ruled by prevalent configurations, normally between 4 to 6 potential maps, that usually remains quasi stable for 80 ms to 120 ms before changing to another map. These maps are called EEG microstates [7][10].

The research carried out in [11] proposed to map these EEG signals to some specific latent spaces grounded into the Laplacian matrix spectrum and outputs a high explained variance of the data into a lower dimension space. In this work, a strain of this spectral microstate theory is assessed for neurocognitive disorders identification. The results are compared to pioneer academic works [3] and well succeeded deep learning applications [12].

2. Materials

The Temple University Hospital EEG (TUH EEG) corpus is, to the best of our knowledge, the largest public EEG dataset (DS) available [13]. From 2002 to 2017, this DS had been updated and, currently, it has more than 30,000 records. The TUH Abnormal (TUAB) EEG corpus, a partition of TUH EEG, consists of 2,383 patients and 2,993 sections (1,595 sections from females), carefully classified by specialists as normal or abnormal. The present work uses two balanced TUAB partitions, here on called Evaluation DS and Tuning DS. The first DS is comprised

of 280 instances (150 normal) and is the same material used in the evaluation of the reference works [3]; and the Tuning DS, which comprises 75 instances classified into two groups: 38 (24 females, age 47.07 ± 17.85) EEG files from healthy patients and 37 (19 females, age 48.94 ± 16.59) EEG files from patients having some kind of mental disorder. However, our approach has a previous unsupervised stage, where a partition of healthy instances from the Tuning DS was previously used for obtaining prototypes of microstates (as demonstrated in [11]) and for training of the classification models.

All the instances used in this work have an Averaged Reference EEG configuration. This means the reading potential of an electrode is referenced to the average of certain group of electrodes measured at A1 and A2, according to the Figure 1.a. Besides these features, the complete DS was preprocessed for meeting generality: 21 channels were kept on every record, as shown in Figure 1.b, and blue dots represent the removed electrodes, FPz and Oz.

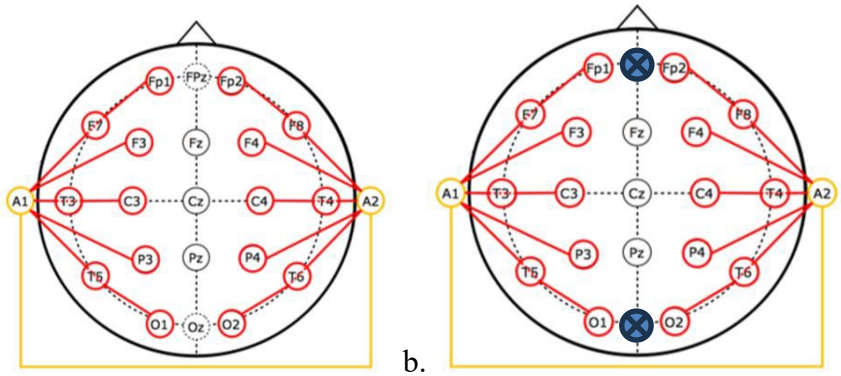

a. b.

Figure 1. AR electrodes configuration: a. TUAB EEG corpus, b. Electrodes selection in this work, adapted from [14].

In the DS, there are several configurations, including varieties in the number of channels for EEG acquisitions, however, the 21 selected channels are often available since the 10-20 system is the most common EGG montage [14]. Besides the selection of channels, all the records have been resampled at 250Hz, this also sets a standard for the work development and eliminates extra routines specifics for different number of channels and sample rates. The public TUH EEG corpus has a previous artifact correction, but the partitions used in this work have been 2-20Hz filtered [10] for meeting the alfa band signal, the quasi-stable region of the microstates [7]. Together with the resampling routine and the band pass filter, all the data treatment was carried out with the aid of the EEG Lab Matalb toolbox®.

3. Methods

3.1. The EEG Microstates Theory

Studies have demonstrated that microstates are easier to determine from EEG signals in the moments of higher potential variation, normally as the electric maps change on the scalp, yielding a higher signal-to-noise ratio [15]. These moments are flagged by the peaks in the standard deviation among the EEG channels, or the Global Field Power (GFP). Therefore, the first step to represent the EEG signal in a microstates series is to compute the GFP, where u_i $(i = 1,2, \dots c)$ is the signal in the ith electrode, of c EEG electrodes, at time sample t, according to Equation 1.

$$GFP_t = \sqrt{\frac{1}{c} \sum_{i=1}^{c} (u_i(t) - \bar{u}(t))^2} \quad (1)$$

Once the patterns at GFP peaks are computed, an unsupervised learning algorithm (normally a modified K-means) is applied to cluster the topographic maps. Four clusters are normally used to represent the EEG signals [10], and their centroids are called microstates prototypes. The Global Explained Variance (GEV) is used to state how much information a set of microstates prototype encompasses from the EEG signal. Equation 2 presents the GEV_n for a given prototype, al_k, $k_i \in K$ (set of prototypes), u_n is the array of electric potentials, N represents the number of time samples in the EEG. This step is important to define the number of microstates that will be used to represent the EEG signal as well as the most appropriate ones.

$$GEV_n = Corr(u_n, al_n)^2 . (GFP_n^2 / \sum_{n'}^{N} GFP_{n'}^2) \quad (2)$$

After defining the microstates prototypes, a procedure called backfitting is performed. In this step, every single scalp topography of electric potential is assigned to some microstate, so that the result is a microstate series. Figure 2 presents the process of representing an EEG signal in a microstate series [10].

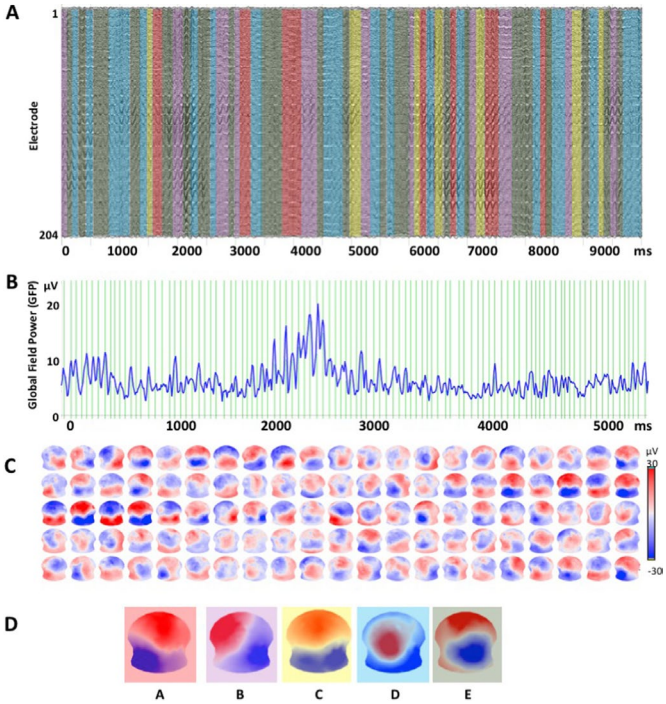

Figure 2. Illustration of the EEG microstate method: A) 10-sec eyes-closed EEG signal; B) GFP curve of the first 5 s of the EEG signal, where the GFP peaks are marked by vertical lines; C) topographic maps at consecutive GFP peaks; and D) microstates prototypes obtained after applying a modified k-means. Then, each time point of the EEG signal is represented by one microstate prototype [10].

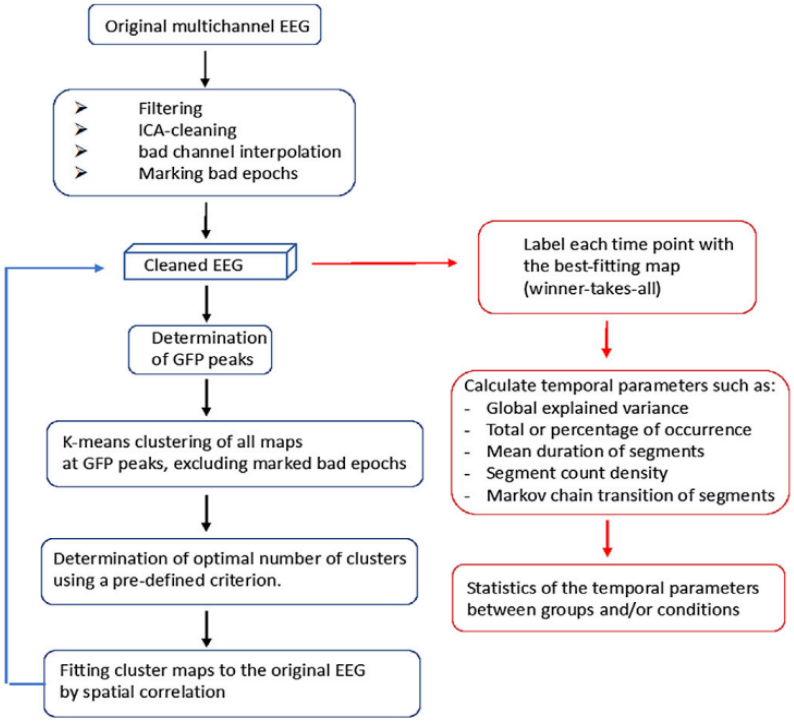

Figure 3. Classic microstate statistic extraction workflow, adapted from [10]

Given the microstates, it is possible to draw the statistics related to the microstates assignment. Five temporal metrics are normally extracted, regarding each microstate: the average duration, frequency of occurrence, coverage, global explained variance, and transition probabilities of a given microstate to the others [10]. Figure 3 presents the classic and yet, commonly used microstate workflow [6][10][15].

3.2. Fundamentals of Spectral Clustering

Spectral clustering is an unsupervised learning algorithm based on the spectral graph theory [17]. It assumes the basic hypothesis that points in the same groups are similar, and points in different groups have weak similarity. Given a set of n patterns $(x_1, x_2, \ldots x_n)$, this technique represents the data in the form of similarity graph (G) of vertices (points) and edges (link between vertices), where the weight between two vertices x_i and x_j is zero ($w_{ij} = 0$) if they are not similar or below some threshold, otherwise, the weight is a positive value $w_{ij} \geq 0$, with $w_{ij} = w_{ji}$. The weighted adjacency matrix of the graph is the matrix W, where each element represents the weight between the vertices, defined by Equation 3 as

$$W = (w_{ij})_{i,j=1,\ldots,n} \tag{3}$$

For the same graph (G), the degree matrix (D) is defined as a diagonal matrix, with degrees $(d_1 \ldots d_n)$ on it, where the degree of a vertex (x_i) represents the number of other vertices (x_j) linked to it, according to Equation 4:

$$d_i = \sum_{j=1}^{n} w_{ij} \tag{4}$$

The vertex degree equation shows the sum only happens over the vertices adjacent to x_i, and zero to any other vertex. For convenience, we can think in a relaxed problem of zeros and ones (vertices connected or not), and a subset of vertices $A \subset V$ (the group of all the vertices in G), and its complement $\bar{A}$. For better understanding, the problem is relaxed instead, therefore the weight between vertices is given by the indicator vector $1_A =$

$(f_1, f_2 \ldots f_n)', \in R^n$, where the entries $f_i = 1$, if $v_i \in A$, and 0, for the complements. Finally, the unnormalized Laplacian matrix (L) is defined by Equation 5:

$$L = W - D \tag{5}$$

In practice, from a matrix of n patterns $X_{c \times n}$ (raw data), turned into a similarity graph G (by approximation), the aforementioned matrices would have the form in Figure 4, according to Equation 5.

$$\mathbf{W} = \begin{bmatrix} 0 & 1 & 1 & 0 & 0 & 0 & 0 \\ 1 & 0 & 1 & 1 & 0 & 0 & 0 \\ 1 & 1 & 0 & 0 & 0 & 0 & 0 \\ 0 & 1 & 0 & 0 & 1 & 1 & 1 \\ 0 & 0 & 0 & 1 & 0 & 1 & 0 \\ 0 & 0 & 0 & 1 & 1 & 0 & 1 \\ 0 & 0 & 0 & 1 & 0 & 1 & 0 \end{bmatrix} \mathbf{D} = \begin{bmatrix} 2 & 0 & 0 & 0 & 0 & 0 & 0 \\ 0 & 3 & 0 & 0 & 0 & 0 & 0 \\ 0 & 0 & 2 & 0 & 0 & 0 & 0 \\ 0 & 0 & 0 & 4 & 0 & 0 & 0 \\ 0 & 0 & 0 & 0 & 2 & 0 & 0 \\ 0 & 0 & 0 & 0 & 0 & 3 & 0 \\ 0 & 0 & 0 & 0 & 0 & 0 & 2 \end{bmatrix} \mathbf{L} = \begin{bmatrix} 2 & -1 & -1 & 0 & 0 & 0 & 0 \\ -1 & 3 & -1 & -1 & 0 & 0 & 0 \\ -1 & -1 & 2 & 0 & 0 & 0 & 0 \\ 0 & -1 & 0 & 4 & -1 & -1 & -1 \\ 0 & 0 & 0 & -1 & 2 & -1 & 0 \\ 0 & 0 & 0 & -1 & -1 & 3 & -1 \\ 0 & 0 & 0 & -1 & 0 & -1 & 2 \end{bmatrix}$$

Figure 4. Weight matrix (W), adjacency matrix (D) and the Laplacian matrix (L), adapted from [19]

Note that the Laplacian matrix (L) has the same values of D on the main diagonal, out of the diagonal, L has -1 if there is a link between nodes of row i and column j, and zero, otherwise. Also, note that the sum of the elements in a row or column always is equal to zero, as the constraint of the Laplacian matrix. It has the form of a diagonal block matrix, with L_i blocks corresponding to the real clusters in the data. Finally, the trick is to explain L by its spectrum since this representation enhances the cluster-properties [17]. This is normally done with the application of Singular Value Decomposition (SVD). The optimal number of singular vectors is defined with the eigengap heuristic, and this is a very special point in this technique, since it may provide an expressive dimension reduction. The last step is the implementation of a clustering algorithm over the remaining singular vectors.

3.3. Spectral Microstates of EEG

The use of spectral clustering theory for extracting microstates from EEG signals is a novel approach, described by da Rocha Junior in [11], that in [11] generated higher GEV than the traditional microstate method. The workflow of this method is presented in Figure 5, where the EEG signals in the instants of GFP peaks are arranged into a $X_{c \times n}$ matrix, being c the number of channels and n the number of time samples.

Initially, the matrices W and D are extracted from de raw dataset, following the Laplacian matrix and its spectrum, also outlined in Section 3.2. Observe that in the spectrum of the Laplacian matrix $S_{m \times n}$, where $m < c$, that is, there is a dimension reduction. Once the data is mapped in this latent space (S), a suitable clustering technique needs to be applied to identify the clusters, which are the prototypes itself, $K = (k_i)_{i=1,\ldots,l}$. We call these prototypes of spectral microstates since they are generated on the L matrix spectrum, and normally identify them by labels (A, B, C, D…). In this work, the technique chosen was the K-medoids, since it is less sensitive to outliers in data, and uses real data as centroids [17].

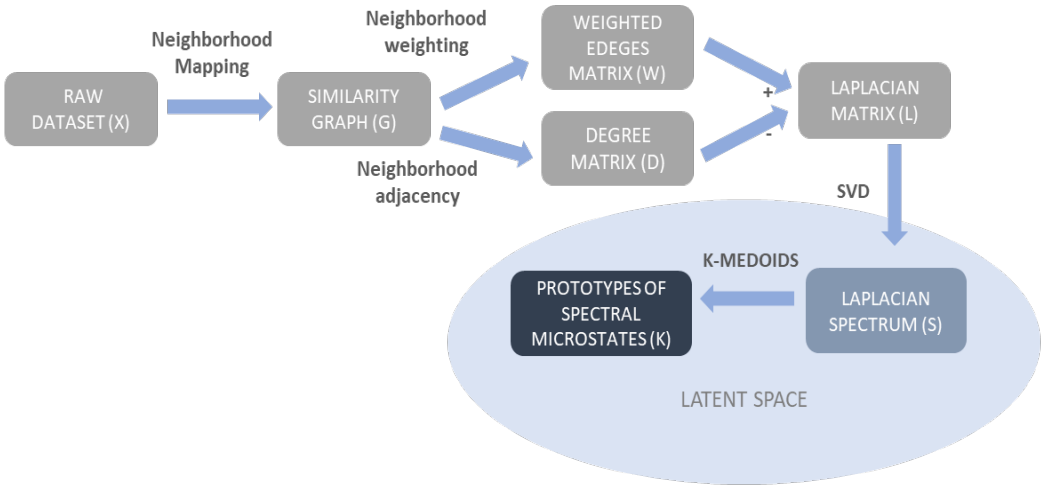

Figure 5. Spectral prototypes of EEG workflow

To assign to each EEG sample a microstate, the workflow in Figure 5 is run as far as the spectrum (*S*') of the new EEG instance, then, the previous prototypes shall be backfitted with the data. Figure 6 illustrates this procedure: the distance metric between the prototypes (*K*) and every sample in (*S*') is calculate; the samples receive the same label of the nearest prototype k_i.

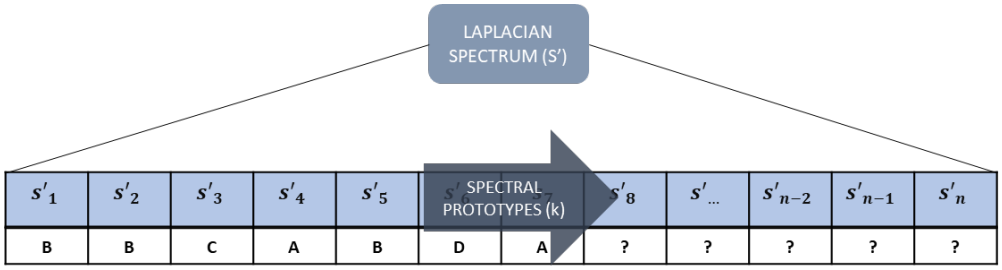

Figure 6. Labeling new EEG step samples with pairwise and spectral prototypes (K)

Normally, the same distance metric used in the prototypes development (*K*) should be used in the pairwise algorithm. Since the *K* and *S'* have been designed from Laplacian matrix spectrums with the same metrics, as an effect of the new mapped space, the prototypes have high generality levels as compared to the samples in the original space [11]. The procedure to assign a microstate to each EEG sample produces a microstates series, and from this series, we can compute the same five temporal metrics of the traditional microstate method, as described in Section 3.1. The result of mapping EEG signals to a microstates series may vary depending on several parameters used in the workflow of Figure 5. The most influential adjustments for the outputs are the metric distance or the similarity measure used for the similarity graph and spectral prototypes, type of similarity graph, dimensions of *S* and *K*, and number of medoids (same as prototypes). The chosen values for these adjustments in this paper were cosine, cosine, complete, 3, and 8, respectively. The result of this workflow, after mapping several EEG records, are columns with each time sample labeled (microstate) and rows of EEG records, as the example presented in Figure 7.

EVERY EEG MAPPED ON THE LATENT SPACE	LABEL ASSIGNED TO EACH TIME SAMPLE						
	1	2	3	...	n-2	n-1	n
s'_1	A	B	D	...	C	C	B
s'_2	D	C	A	...	B	A	D
s'_3	C	A	B	...	C	C	B
...	...	...	...	...	...	...	...
s'_{m-2}	B	A	D	...	A	A	C
s'_{m-1}	A	B	B	...	D	A	D
s'_m	A	C	C	...	A	B	B

Figure 7. EEG records mapped in the latent space of Laplacian matrix (rows) and microstates labeled according to the prototypes (columns)

The classic approach for microstate analysis uses statistical features of the labeled series *S'*, as mentioned in Section 3.1. Since the novelty in this work is focused on the preprocessing stage, ordinaries machine learning models were applied to distinguish normal from abnormal groups based on the following statistics: the time fraction of the signal each microstate is activated (coverage), the frequency of each microstate occurs in the signal (individual frequency), the average period a microstate remains active as it occurs (duration), and overall transition probability (shifting frequency).

4. Experiments and Results

To evaluate the presented approach, the healthy instances from the Tuning DS, presented in Section 2, was initially used for producing models of microstates (8 prototypes). 10 seconds of each EEG file were drawn and read at the GFP peaks, arranged into an $X_{c \times n}$ matrix, where c is the number of channels and n is the number of time samples.

After obtaining the prototypes, the Tuning and the Evaluating DS passed through the workflow presented in Section 3.3, they were represented as sequences of microstates (Figure 6), and 25 features were computed for 10 seconds of each EEG in the Tuning and the Evaluation DS (3 features for each prototype and one for the overall probability of transition), the statistics are computed and used for supervised learning. These 75 instances statistics from Tuning DS were split in 85/15 for training and tuning classic supervised learning models for classification of normal and abnormal EEGs. First, two algorithms (KNN and SVM) were tried with aid of the Bayesian Optimization over the Tuning DS, with minimization of the five-fold loss for the likely best parameters. After the Bayesian optimization suggestion, the proposed models were evaluated with 30 different random seeds for cross-validation partition and random initialization, for testing results stability. The third model was a feedforward net, its architecture was drawn by the multiple interaction search with variation of the last hidden layer (from 2 to 50 neurons). The three models with the least mean error (Equation 6) were used in the test phase for 30 new random simulations using the 280 instances of the Evaluation DS. The evaluations were taken according to the mean error:

$$\varepsilon = \frac{N_e}{N_t} \times 100\% \tag{6}$$

where N_e is the number of incorrect classification samples and N_t is the total amount of samples in the partition.

Three machine learning algorithms for classification were used in the experiments:

- K Nearest Neighbors (KNN) – Euclidean distance and 1 neighbor.

- Support Vector Machines (SVM) – Order 3, polynomial kernel, boxconstraint 0.041 and kernel scale 0.640.
- Artificial Neural Network (ANN) – feedforward net 4/10/41 neurons (tansig/tansig/logsig transfer functions).

Table 1 shows the mean and standard deviation of error after 30 iterations of each algorithm on each phase when using the presented methodology.

Table 1. Models error rate (%) and standard deviation (%) on each development phase

Model	Test	STD
KNN	26.07	0.01%
SVM	24.57	7.54%
ANN	**12.50**	19.90%

It was important to apply the KNN and SVM algorithms for comparing with other works [3][5] that used the same models and check the specific effect of the preprocessing techniques. The SVM model has excelled KNN with a 24.57% error rate, but both systems have exceeded other works. However, the ANN model has presented a mean error of 12.50%, which exceeded the other approaches (see Table 2), without the usage of any deep network architectures. This baseline results are better than the CNN used in [3], but under the results of the WaveNet-LSTM application [12]. Despite the variation for the standard deviation, 19.90%, during the interactions for searching for the best model, several other architectures have presented prominent results as well.

The reference works have used a larger training set (2785 instances) from the TUAB corpus, while in this work, we have used only 75 instances of the same corpus, however, this research used the same partition for the models' evaluation (280 instances). These facts strengthen the reliability of the spectral microstates approach for the task assigned in this work. Table 2 summarizes our results compared to the reference works.

Table 2. Models error rate (%) comparation

Study	Mean Error	Model
Lopez et al.[3]	21.20%	CNN-MLP
Albaqami et al.[12]	**11.24**	WaveNet-LSTM
Our work	12.50	Feedfoward Net

5. Conclusions

In this work, we presented an approach called spectral EEG microstates and we applied it to the detection of patients with mental disorders. Different from the traditional EEG microstates method, the new approach obtains the EEG microstates using spectral clustering theory. In our experiments, a neural network obtained a mean error of 12.50% using few training instances. This result was similar to those obtained by more complex neural networks, which used much more training instances. These observations suggest the efficiency of the spectral microstates technique and support future works with larger datasets and the application of deep architecture techniques, like neural networks applied directly over the streaming of microstates (Figure 6) and automatic extracting of features for classification, aiming for better results and assistance with clinical diagnosis.

Acknowledgements

The authors thank the financial support for the research from the project of the Conselho Nacional de Desenvolvimento Científico e Tecnológico (CNPq) and Fundação de Amparo à Pesquisa do Espírito Santo (FAPES), number 598/2018.

References

[1] Park, S. M., Jeong, B., Oh, D. Y., Choi, C.-H., Jung, H. Y., Lee, J.-Y., Lee, D., & Choi, J.-S. (2021). Identification of major psychiatric disorders from resting-state electroencephalography using a machine learning approach. Frontiers in Psychiatry, 12, 707581.

[2] Pascual-Marqui, R. D., Michel, C. M., & Lehmann, D. (1995). Segmentation of brain electrical activity into microstates: model estimation and validation. IEEE Transactions on Biomedical Engineering, 42(7), 658-665.

[3] López, S., Obeid, I., & Picone, J. (2017). Automated interpretation of abnormal adult electroencephalograms (Doctoral dissertation).

[4] Alves, L. M., Côco, K. F., de Souza, M. L., & Ciarelli, P. M. (2020, December). Graph Theory Analysis of Microstates in Attention-Deficit Hyperactivity Disorder. In Congresso Brasileiro de Automática-CBA (Vol. 2, No. 1).

[5] Ku, D. W., & Ciarelli, P. M. (2021, October). Classificação Automática de Sinais Anormais de EEG por meio de Microestados e Aprendizado de Máquina. In Simpósio Brasileiro de Automação Inteligente-SBAI (Vol. 1, No. 1).

[6] Poulsen, A. T., Pedroni, A., Langer, N., & Hansen, L. K. (2018). Microstate EEGlab toolbox: An introductory guide. BioRxiv, 289850.

[7] Lehmann, D., Strik, W. K., Henggeler, B., König, T., & Koukkou, M. (1998). Brain electric microstates and momentary conscious mind states as building blocks of spontaneous thinking: I. Visual imagery and abstract thoughts. International Journal of Psychophysiology, 29(1), 1-11.

[8] Gschwind, M., Hardmeier, M., Van De Ville, D., Tomescu, M. I., Penner, I.-K., Naegelin, Y., Fuhr, P., Michel, C. M., & Seeck, M. (2016). Fluctuations of spontaneous EEG topographies predict disease state in relapsing-remitting multiple sclerosis. NeuroImage: Clinical, 12, 466–477.

[9] Zhao, Y.-N., He, J.-K., Wang, Y., Li, S.-Y., Jia, B.-H., Zhang, S., Guo, C.-L., Zhang, J.-L., Zhang, G.-L., Hu, B., Fang, J.-L., & Rong, P. (2022). The pro-inflammatory factors contribute to the EEG microstate abnormalities in patients with major depressive disorder. Brain, Behavior, & Immunity - Health, 26, 100523.

[10] Michel, C. M., & Koenig, T. (2018). EEG microstates as a tool for studying the temporal dynamics of whole-brain neuronal networks: a review. Neuroimage, 180, 577-593.

[11] da Rocha Junior, V., & Ciarelli, P. M. (2022). Fundamentals of Spectral Clustering for Extracting Microstates of EEG. In: IX Congresso Latino-Americano de Engenharia Biomédica (Claib).

[12] Albaqami, H., Hassan, G. M., & Datta, A. (2023). Automatic detection of abnormal eeg signals using wavenet and lstm. Sensors, 23(13), 5960.

[13] Harati, A., Lopez, S., Obeid, I., Picone, J., Jacobson, M. P., & Tobochnik, S. (2014, December). The TUH EEG CORPUS: A big data resource for automated EEG interpretation. In 2014 IEEE signal processing in medicine and biology symposium (SPMB) (pp. 1-5). IEEE.

[14] Ferrell, S., Mathew, V., Refford, M., Tchiong, V., Ahsan, T., Obeid, I., & Picone, J. (2020). The Temple University Hospital EEG corpus: Electrode location and channel labels. Institute for Signal and Information Processing Report, 1(1).

[15] Lehmann, D., Strik, W. K., Henggeler, B., König, T., & Koukkou, M. (1998). Brain electric microstates and momentary conscious mind states as building blocks of spontaneous thinking: I. Visual imagery and abstract thoughts. International Journal of Psychophysiology, 29(1), 1-11.

[16] Lehmann, D., Pascual-Marqui, R. D., & Michel, C. (2009). EEG microstates. Scholarpedia, 4(3),7632.

[17] Von Luxburg, U. (2007). A tutorial on spectral clustering. Statistics and computing, 17, 395-416.

[18] Park, H. S., & Jun, C. H. (2009). A simple and fast algorithm for K-medoids clustering. Expert systems with applications, 36(2), 3336-3341.
[19] Albanie, S. (2019). Euclidean distance matrix trick. Retrieved from Visual Geometry Group, University of Oxford.